Optics Communications 283 (2010) 1684–1689

Contents lists available at ScienceDirect

Optics Communications

journal homepage: www.elsevier.com/locate/optcom

3D refractive index profile for the characterization of necking phenomenon along stretched polypropylene fibres

A.A. Hamza [a], T.Z.N. Sokkar [b], M.A. El-Morsy [c], M.I. Raslan [b], A.M. Ali [b,*]

[a] British University, El Sherouk City, Egypt
[b] Physics Department, Faculty of Science, Mansoura University, Mansoura, Egypt
[c] Physics Department, Faculty of Science (Damietta), Mansoura University, Damietta, Egypt

ARTICLE INFO

Article history:
Received 6 August 2009
Received in revised form 22 December 2009
Accepted 22 December 2009

Keywords:
Refractive index profile
Necking
Polypropylene
Orientation function

ABSTRACT

The phenomenon of neck formation in polymers has attracted considerable attention. During the cold-drawing process an initial undrawn material is transformed into anisotropic one across a narrow transition region called 'neck'. The Video Opto-Mechanical (VOM) device attached with multiple-beam Fizeau fringes techniques are used to stretch polypropylene (PP) fibres. A iPP sample is stretched to have a neck at room temperature. The optical properties of the deformed material over the necking region are examined. Another PP sample is stretched (without necking deformation) at room temperature and the optical properties are also examined. The task of this study is to characterize and assess the necking phenomenon along cold-drawn polypropylene (iPP) fibre axis. The effect of necking on the optical properties of the fibre is confirmed by the determination of the 3D refractive index profile at different regions along the deformed PP fibre. Also the orientation function is calculated for the necked sample. The contour lines of microinterferograms are given for illustrations.

1. Introduction

Optical measurement is based on the wave characteristics of light when it reflects from or transmits through an object. Light transmission properties through a fibre depend mainly on its refractive index profile and material dispersion. The refractive index profile of optical or textile fibres is important not only in assessing the performance of the fibre in a given system but also it helps in fibre fabrication to improve its products. Therefore, increasing need for fast and accurate measurement of refractive index profile of fibres because it provides information for the correlation between their structure and the other properties. One of the most sensitive and non-destructive techniques, used to obtain this information, is multiple-beam Fizeau fringe system. So, this technique has been successfully used to investigate textile and optical fibres [1–5]. Sokkar et al. [6] created a software programme to determine the refractive indices and birefringence of PP fibre.

Studying the mechanisms of micro-deformation in polymers is used to establish connections between the macroscopic toughness and molecular parameters to enhance the design of new materials with improved properties [7]. Most synthetic textile fibres are manufactured with no desirable tensile properties and having low birefringence. The synthetic textile fibres should be drawn out to make them thinner, stronger and consequently more birefringent fibres in order to turn them into useful textile fibres [8].

The necks in polymers, were first observed about 70 years ago [9], and are now commonly used in modern processing of polymer films and fibres. Hamza et al. investigated interferometrically the structural deformation occurs in polypropylene fibre when it is stretched at low draw ratios [10] in the case of fast and slow cold drawing. They detected two mechanisms of deformation, one of them is the smooth deformation and another one is necking deformation which is detected when the PP fibre is stretched with fast drawing. Sokkar et al. [11] designed a Video Opto-Mechanical (VOM) device to characterize the online drawing process. They detect the threshold speed to avoid necking occurrence.

For semi-crystalline polymers, such as PP fibres, yielding and cold drawing contain two types of non-uniform deformation processes. The first one is the initiation of local necking and the other is the propagation of neck shoulders along the specimen. The local instability of deformation leads to the formation of the above mentioned deformations [12]. Polypropylene sample was stretched to necking at room temperature and the morphologies of the deformed material over the necking region were examined with SEM and TEM [13].

Necking diffusion process has received much attention. Several authors like G'Sell et al. [14] proved that the kinetics of neck formation and propagation could be modeled and predicted from

* Corresponding author. Address: Physics Department, Faculty of Science, Mansoura University, Elgomoheria Street, Mansoura, Egypt.
E-mail address: Afaf_maweed@mans.edu.eg (A.M. Ali).

0030-4018/$ - see front matter © 2009 Elsevier B.V. All rights reserved.
doi:10.1016/j.optcom.2009.12.059

the constitutive equation of the material expressed in terms of true stress, strain and strain rate. Chudnovsky and Preston [15] formulated of metric Lagrangian model that based on understanding the necking phenomena. It has been reported that the onset of necking takes place when the true stress reaches certain constant value independent of the applied load.

This work throws light on the interferometric detection and characterization of the necking phenomenon along iPP fibres using multiple-beam Fizeau fringes technique. A sample of iPP fibre is cold drawn to a draw ratio DR = 1.5 with necking deformation. Another sample of iPP is cold drawn to DR = 1.5 without necking formation. The 3D profile of refractive indices and orientation function are determined to clarify the effect of necking.

2. Necking in polymer fibres

The necking formation has attracted considerable attention. Necking was formed due to the transformation of crystalline regions under the applied stress, until it was observed to occur also in amorphous polymers [16]. An early interpretation was declared the neck appearance as a result of the thermal softening produced from the localized heating. But it was later demonstrated that necking could occur under certain isothermal conditions. Both of the above interpretation can be involved in the necking formation process and will influence its propagation. But they are not necessarily responsible for its initiation [16]. Necking is the manifestation of instability in the yielding process due to defects on a molecular level. The defects on the macroscopic level in the material acts as areas of stress concentration (cf. Ref. [16]).

Recently, Hamza et al. [10] reported that the necking in PP fibres occurred due to the mechanical weak bonds, the formation of voids or pores within the fibre structure, microscopic inhomogeneities and, a large extent for the oriented polymer molecules. Experimentally during the cold drawing, the necking deformation appears at different regions along the fibre axis when the heating rate of these regions exceeds the limit of flowing temperature of the molecular chains. Where the cold-drawing process associated with the release of quantity of heat that is equivalent to the work done on the fibre, a part of this heat leads to heating the fibre and the other part is dissipated into the surrounding [17].

The temperature rise at the neck region has been studied mainly by two methods. The first method is a calorimetric method to measure the total heat generated during necking. The second method measures the temperature rise directly by an infrared camera. Both the methods indicate appreciable increase in temperature; in some cases, it has been reported that temperature rises up to 90 °C from room temperature [18].

3. Results and discussion

Sokkar et al. [11] designed a Video Opto-Mechanical device (VOM) in order to determine dynamically the mechanical, optical and structural properties of fibres at different uniform stretching speed. The VOM device attached with multiple-beam interferometric system is an accurate and efficient technique in the field of interferometery applied for monetring of fibres. The setup of VOM [11] used in this work is shown in Fig. 1. This device consists of three basic units namely interferometric, mechanical and computerized.

A sample of undrawn iPP fibre with a certain length is fixed from its ends with the two gear boxes and mounted on the lower optical flat of the wedge interferometer. The fibre filament is immersed in a suitable liquid with refractive index $n_L = 1.5041$, at temperature ($T = 30$ °C). The mechanical system is transferred to the optical microscope stage. The wavelength of monochromatic light used is 546.1 nm. This wedge interferometer is adjusted in such a way that the fibre axis is exactly perpendicular to the interference fringes in the liquid region. The iPP fibres are stretched by two different stretching speeds. The first speed (slow stretching process) is selected to be less than the threshold speed [11] at which the necking deformation did not occur. The second speed (fast stretching process) is selected to obtain a deformed necked sample. In the previous work [11] it is recommended the PP fibres must be stretched slowly with low speed to avoid the occurrence

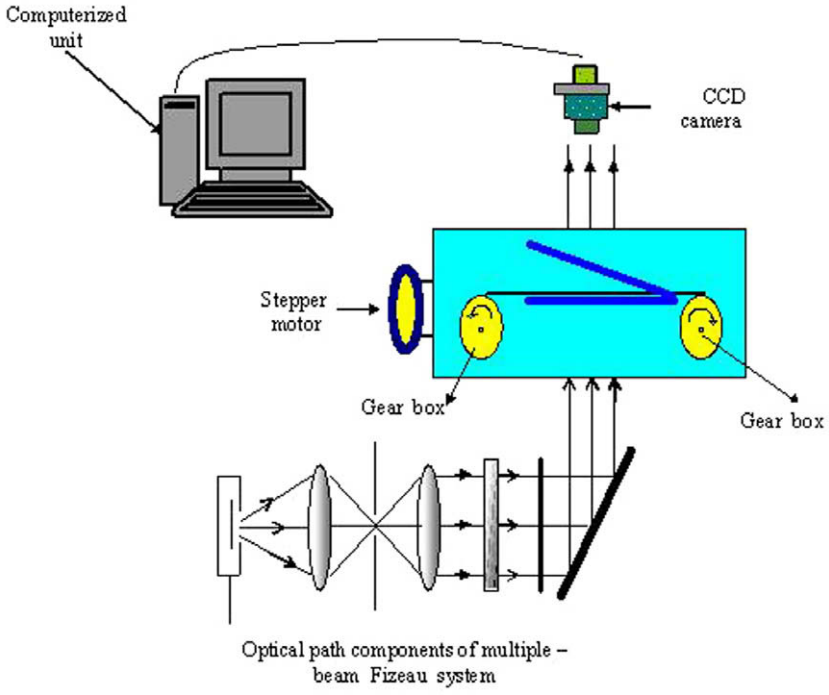

Fig. 1. A schematic diagram of the used VOM device.

of necking deformation, which occur during stretching with high speed (fast stretching). The speed that must be avoided is ($V > 0.298$ cm/s). So the sample that stretched with low stretching speed lower than the threshold speed does not show necking while the other one that stretched with higher speed than V_{th} shows necking.

In the case of slow stretching process the stepper motor speed is adjusted to be $V = 0.1$ cm/s. But for fast stretching process the stepper motor speed is adjusted to be $V = 0.745$ cm/s. Two samples of undrawn iPP fibres are drawn to draw ratio DR = 1.5 with the above selected two speeds. The obtained images are recorded by using the CCD camera. Fig. 2a shows the obtained contour lines of the microinterferogram of undrawn iPP (DR = 1) when light vibrating parallel to the fibre axis. Fig. 2b shows the obtained contour lines of the microinterferogram of drawn iPP (DR = 1.5) with speed $V = 0.1$ cm/s when light vibrating parallel to the fibre axis. The fringe shifts or the contour lines in Fig. 2a and b are remarked to be easy for the identification of the optical and geometrical properties along the fibre axis. The contour line for each remarked fringe along the fibre axis show that, there is no significant change in the fringe shifts inside the iPP fibres.

3.1. Interferometric study of neck deformation zone

The necking phenomenon usually occurs when a homogeneous polymeric fibre is stretched uniaxially. In this case the polymer fibre is not deformed homogeneously. Instead, two almost uniform sections occur in the sample: the two sections being nearly equal to its initial thickness. These sections are jointed by a relatively short transition (necking) zone that propagates with a constant speed along the fibre. Fig. 3a shows the obtained contour lines of microinterferogram of drawn iPP (DR = 1.5) with speed $V = 0.745$ cm/s. When light vibrating parallel to the fibre axis. Fig. 3b is a schematic diagram of drawn fibre containing a neck zone. This diagram can be classified into three microscopic regions according to the morphological model of Shimizu et al. [19] and the molecular model of Peterlin [17]. The 'as spun' part of fibre (before neck) may be identified as 'oriented mesophase', the neck shoulder (neck zone) as 'super drawing' and drawn fibre part (after neck) as 'completion of crystallization and molecular orientation'.

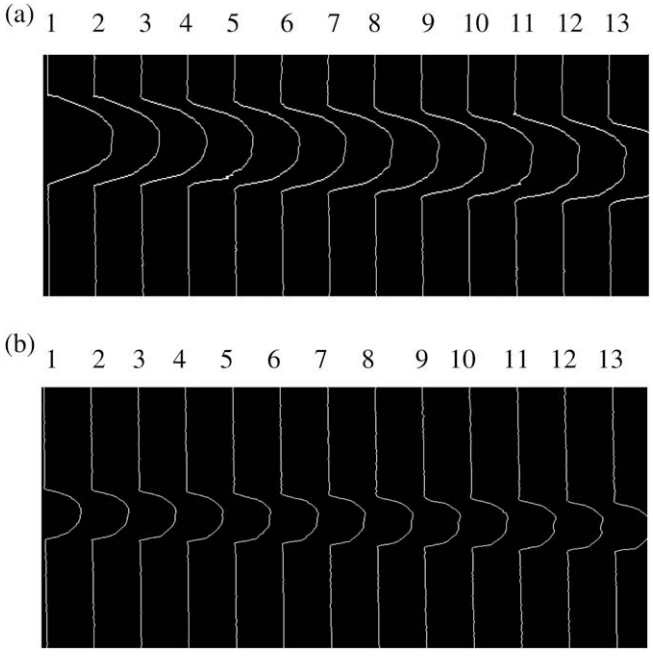

Fig. 2. The contour lines of microinterferogram for light vibrating parallel to the fibre axis (a) for undrawn PP fibre and (b) for cold-drawn PP fibres in case of slow stretching.

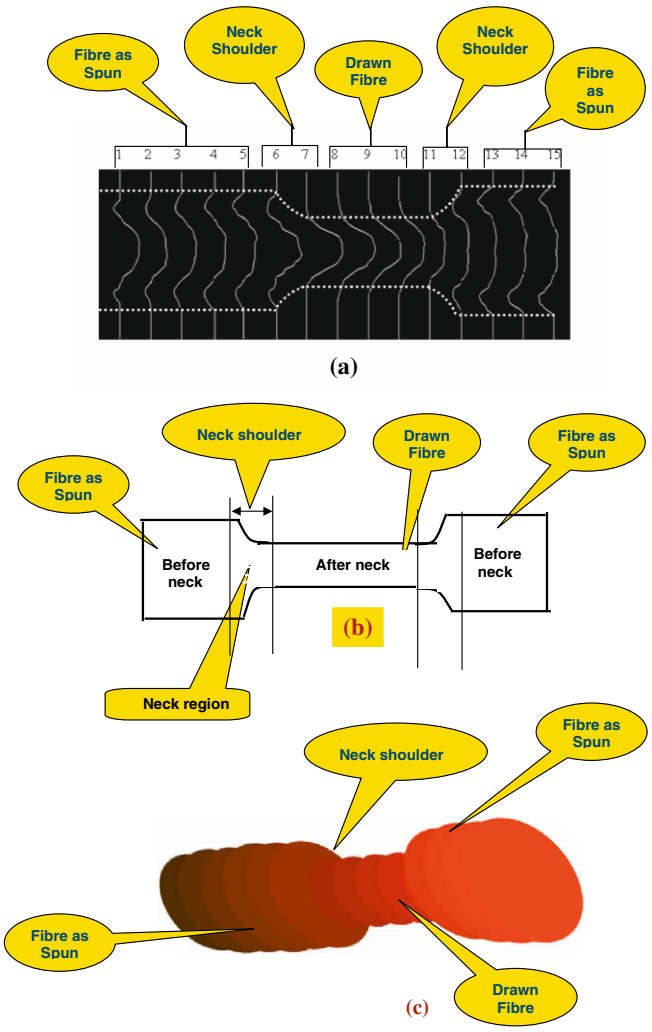

Fig. 3. (a) The contour lines of microinterferogram of cold-drawn PP fibre for light vibrating parallel to the fibre axis in case of fast stretching process, (b) a schematic diagram of drawn fibre containing a neck deformation zone and (c) the 3D profile of the fibre thickness for PP fibres.

In Fig. 3a, the fringe shifts are remarked to be easy for the identification of the optical and geometrical properties along the fibre axis. The contour lines of microinterferogram shown in this Figure can be interpreted basically on morphological model [19] and molecular model [17] as follows: (i) in the oriented mesophase; the displacements of fringe shifts (1, 2, 3, 4, 5, 13, 14 and 15) inside the fibre are relatively small, this means that the fibre is slightly drawn, has larger thickness. (ii) In the super drawing; the displacements of fringe shifts (6, 7, 11 and 12) inside the fibre are longer than that of oriented mesophase region, this means that the fibre is super drawn, has gradient thickness. (iii) In the completion of crystallization and molecular orientation; the displacements of fringe shifts (8, 9, and 10) inside the fibre are relatively longer compared to the previous two regions, this means that the fibre is highly drawn compared with the fibre as spun zone and has smaller thickness. Fig. 3c shows the 3D profile for the thickness of drawn iPP fibre. It is clear from Fig. 3c that the fibre thickness has been changed greatly along fibre axis proving the existence of necking deformation. The fibre thickness for fringe shifts (1, 2, 3, 4, 5, 13, 14 and 15) is about 58 μm, the fibre thickness for fringe

shifts (6, 7, 11 and 12) is about 49 μm and the thickness for fringe shifts (8, 9, and 10) is about 31 μm. This figure and the contour lines of the microinterferograms in Fig. 3a strongly confirm the morphological and molecular models [17,19].

3.2. 3D refractive index profile

The refractive index n of the fibre can be measured interferometrically by the following equations [3]:

$$\frac{\lambda}{4b}Z = \sum_{Q=1}^{m}(n_Q - n_{Q-1})\left(r_Q^2 - x^2\right)^{\frac{1}{2}} \quad (1)$$

where Z is the fringe shift displacement related to the value x along the radius of the fibre. λ is the wavelength of the monochromatic light used and b is the interfringe spacing. m is the number of the fibre layers. r is the radius of the fibre layer chosen. The refractive index profile is the variation of refractive index across the fibre diameter. The above equation is used to determine the refractive index profile of the fibre. The 3D refractive index profile, which presents accurate measurements of the refractive index across the fibre diameter, was determined. Figs. 4 and 5 represent these 3D refractive index profiles of $n^{\parallel}$ for undrawn sample DR = 1 and drawn sample with draw ratio DR = 1.5 (slow stretching), respectively. In this case of slow stretching there is no variation in the fringe shifts (having the same shape) along the fibre axis. Therefore the refractive index profiles for each fringe shift have nearly the same behaviour as shown in Fig. 5. Fig. 6 represents the 3D refractive index profile for $n^{\parallel}$ of iPP fibre with draw ratio DR = 1.5 (fast stretching). Fig. 6 shows that there is a significant variation in the 3D refractive index profile at different positions along the fibre axis. These variable profile groups are established may be due to the random formation of voids or pores within the fibre structure, which are caused by the necking deformation along the fibre axis [20,21]. In Figs. 4–6 the 3D refractive index profiles are calculated for every fringe shift of the obtained microinterferograms.

To confirm the effect of necking on the structure of PP fibres the orientation function is calculated.

3.3. Orientation function profiles

Molecular orientation is a phenomenon unique to polymers. The degree of molecular orientation of polymers is mostly depending on the Herman's orientation factor (parameter) that relates between the oriented (mean) birefringence B and the intrinsic (maximum) birefringence B_{max} as follows (cf. Ref. [22]):

$$F(\theta) = \langle P_2(\theta)\rangle = \frac{B}{B_{max}} \quad (2)$$

The value of B_{max} for polypropylene fibre is taken to be 0.045 [22]. Table 1 gives the values of orientation function calculated from the microinterferograms of undrawn PP fibre with the aid of Eq. (2). It is clear that the orientation function is constant along the fibre axis.

Cold drawing of a semi-crystalline polymer involves initially the deformation of the spherulitic structure, the subsequent transformation of the spherulitic structure to a fibrillar structure and finally the plastic deformation of the fibrillar structure [17]. Using Eq.

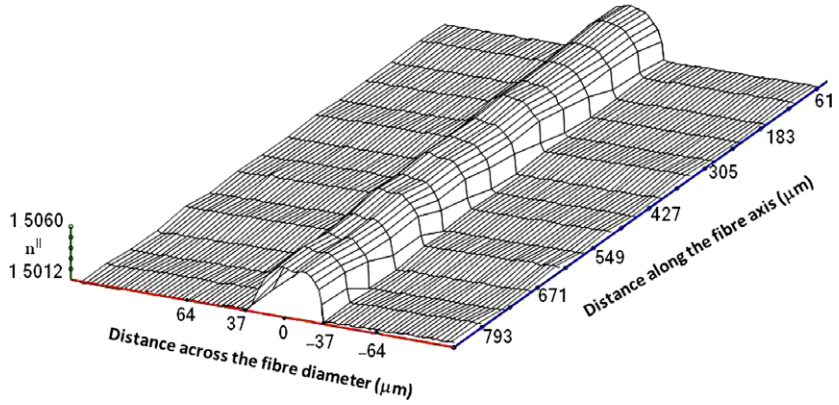

Fig. 4. The 3D refractive index profile for $n^{\parallel}$ for undrawn PP fibre sample DR = 1.

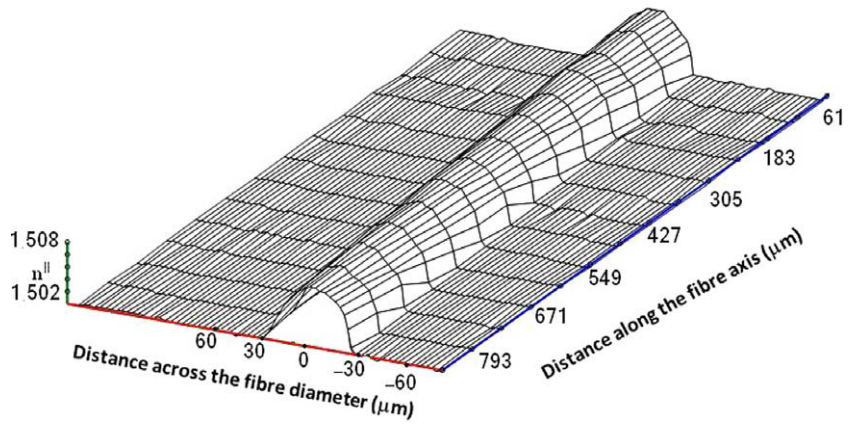

Fig. 5. The 3D refractive index profile of $n^{\parallel}$ of drawn PP fibre sample (DR = 1.5) (slow stretching).

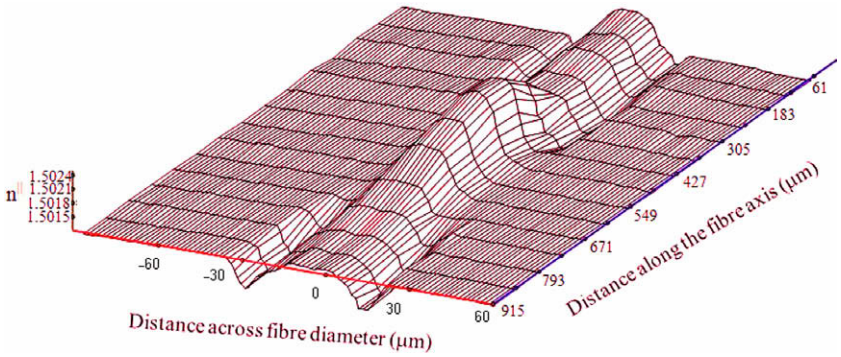

Fig. 6. The 3D refractive index profile of $n^{\parallel}$ at draw ratio DR = 1.5 (fast stretching).

Table 1
The orientation function for undrawn (iPP) fibre.

Fringe numbers	$F(\theta)$
1	0.124
2	0.124
3	0.124
4	0.124
5	0.124
6	0.124
7	0.124
8	0.124
9	0.124
10	0.124
11	0.124
12	0.124
13	0.124

(2) the degree of orientation function is calculated for a necked PP sample in case of fast drawing (V = 745 cm/s) with draw ratio DR = 1.5. Table 2 gives the calculated orientation function shown on the basis of the classification molecular model for a necked sample. It is obvious that the fibre structure suffers deformation during the drawing process along the fibre axis at draw ratio DR = 1.5. The orientations of lamella changes during the morphological transformation from spherulitic structure into fibre structure [17]. In the neck itself a gradual transition from the former into the latter morphology is observed and also a gradual change in the orientation function. The calculated values can be classified into three regions depending on the values of $F(\theta)$ and the molecular model [20,17]. In regions (oriented mesophase (1)) which corresponds to fringe nos. (1–5) and (13–15), respectively in Fig. 3a, the orientation function $F(\theta)$ having lower values. The second region (super drawn or neck shoulder (2)), that corresponding to the fringe nos. 6, 7, 11, 12 in Fig. 3a, it is clear that $F(\theta)$ having higher values than the first region. While in the third region (drawn fibre or after neck) that corresponding to the fringe nos. 8–10 in Fig. 3a, it is clear that $F(\theta)$ having highest values. This indicates that the molecules constituting the fibres at the after neck zone are highly oriented (more birefringent) during the cold-drawing process.

Table 2
The orientation function for cold-drawn (PP) fibre with necking deformation.

Fringe numbers	$F(\theta)$
1	0.134
2	0.134
3	0.134
4	0.134
5	0.134
6	0.135
7	0.135
8	0.263
9	0.281
10	0.277
11	0.135
12	0.135
13	0.134
14	0.134
15	0.134

Peterlin [17] mentioned that the final fibre structure (after neck zone) is characterized by the nearly perfect orientation of chains. From the calculated data for orientation function to after neck zone it is clear that the principle given by Peterlin [17] has been clarified. The obtained values of orientation function in Table 2 strongly confirm the molecular model [17,19].

4. Conclusion

Along side with the well-known techniques such as SEM and X-ray, interferometry is still valuable tool for characterizing the structural deformation of polymer fibres. In the course of cold drawing of polymer fibres, the necking deformation became an expected phenomenon. The refractive index and birefringence values of fibre are considered a micro-detector for optimising the influence of necking phenomenon on the drawing of polymer fibres. This necking is well characterized via the 3D profile for refractive index. The microinterferograms obtained by online multiple-beam Fizeau fringes technique give us a good chance to confirm the identification of neck phenomena of cold-drawn fibre explained by morphological and molecular theoretical models [17,19].

Acknowledgement

We would like to express our deep thanks to Dr. M.A. El-Bakary for his useful discussions.

References

[1] A.A. Hamza, T.Z.N. Sokkar, M.A. Mabrouk, A.M. Ghandar, W.A. Ramadan, Pure Appl. Opt. 3 (1994) 943.
[2] M.A. Mabrouk, M.A. Shams-Eldin, Pure Appl. Opt. 5 (1996) 929.
[3] A.A. Hamza, M.A. Kabeel, J. Phys. D: Appl. Phys. 19 (1986) 1175.
[4] S. Tolansky, Multiple-beam Interferometry of Surfaces and Films, Clarendon Press, Oxford, UK, 1948.
[5] N. Barakat, A.A. Hamza, A.S. Gonied, Appl. Opt. 24 (1985) 4383.
[6] T.Z.N. Sokkar, H.M. El-Dessouky, M.A. Shams-Eldin, M.A. El-morsy, Opt. Laser Eng. 45 (2007) 431.
[7] B. Brulea, H.H. Kauschb, L. Monneriea, C.J.G. Plummerc, J.L. Halarya, Polymer 44 (2003) 1181.
[8] A.H. Gaur, H. De Vries, J. Polym. Sci. 13 (1975) 835.
[9] W.H. Carothers, J.W. Hill, J. Am. Chem. Soc. 54 (1932) 579.
[10] A.A. Hamza, T.Z.N. Sokkar, K.A. El-Farahaty, M.A. El-Morsy, H.M. El-Dessouky, Opt. Laser Technol. 37 (2005) 532.

[11] T.Z.N. Sokkar, M. EL-Tonsy, M.A. EL-Bakary, M.A. El-morsy, A.M. Ali, Opt. Laser Technol. 41 (3) (2009) 310.
[12] E. Kontou, P. Farasoglou, J. Mater. Sci. 33 (1998) 147.
[13] J.X. Li, W.L. Cheung, C.M. Chan, Polymer 40 (13) (1999) 3641.
[14] C. G'Sell, J.M. Hiver, A. Dahoun, Int. J. Solids Struct. 39 (2002) 3857.
[15] A. Chudnovsky, S. Preston, Mech. Res. Commun. 29 (2002) 465.
[16] D.R. Salem, Structure Formation in Polymeric Fibers, Hanser Gardner Publications, Munich, Germany, 2001 (Chapter 2).
[17] A. Peterlin, J. Mater. Sci. 6 (1971) 490.
[18] Akihiko Toda, Chiyoko Tomita, Masamichi Hikosaka, Yu Hibini, Hideki Miyaji, Chisato Nonomura, Toshitake Suzuki, Hideaki Ishihara, Polymer 43 (2002) 947.
[19] J. Shimizu, N. Okui, T. Kikutani, in: A. Ziabicki, H. Kawai High (Eds.), Speed Fiber Spinning, Wiley, New York, 1985, p. 173.
[20] J. Walker, Sci. Am. (1990) 100.
[21] M. Sova, M. Raab, M. Sližová, J. Mater. Sci. 28 (1993) 6516.
[22] D.A. Hemsley, Applied Polymer Light Microscopy, Elsevier Science, Amsterdam, 1989, p. 94.